

A high-performance rechargeable Li-O_2 battery with quasi-solid-state electrolyte

Jia-Yue Peng(彭佳悦), Jie Huang(黄杰), Wen-Jun Li(李文俊), Yi Wang(王怡), Xiqian Yu(禹习谦), Yongsheng Hu(胡勇胜), Liquan Chen(陈立泉), Hong Li(李泓)

Citation: Chin. Phys. B . 2018, 27(7): 078201. **doi:** 10.1088/1674-1056/27/7/078201

Journal homepage: http://cpb.iphy.ac.cn; http://iopscience.iop.org/cpb

What follows is a list of articles you may be interested in

Tuning hybrid liquid/solid electrolytes by lowering Li salt concentration for lithium batteries

Wei Yang(杨伟), Qi-Di Wang(王启迪), Yu Lei(雷宇), Zi-Pei Wan(万子裴), Lei Qin(秦磊), Wei Yu(余唯), Ru-Liang Liu(刘如亮), Deng-Yun Zhai(翟登云), Hong Li(李泓), Bao-Hua Li(李宝华), Fei-Yu Kang(康飞宇)

Chin. Phys. B . 2018, 27(6): 068201. **doi:** 10.1088/1674-1056/27/6/068201

Enhanced ionic conductivity in LAGP/LATP composite electrolyte

Shi-Gang Ling(凌仕刚), Jia-Yue Peng(彭佳悦), Qi Yang(杨琪), Ji-Liang Qiu(邱纪亮), Jia-Ze Lu(卢嘉泽), Hong Li(李泓)

Chin. Phys. B . 2018, 27(3): 038201. **doi:** 10.1088/1674-1056/27/3/038201

Gas treatment protection of metallic lithium anode

Wen-jun Li(李文俊), Quan Li(李泉), Jie Huang(黄杰), Jia-yue Peng(彭佳悦), Geng Chu(褚赓), Ya-xiang Lu(陆雅翔), Jie-yun Zheng(郑杰允), Hong Li(李泓)

Chin. Phys. B . 2017, 26(8): 088202. **doi:** 10.1088/1674-1056/26/8/088202

Conductivity and applications of Li-biphenyl-1, 2-dimethoxyethane solution for lithium ion batteries

Geng Chu(褚赓), Bo-Nan Liu(刘柏男), Fei Luo(罗飞), Wen-Jun Li(李文俊), Hao Lu(陆浩), Li-Quan Chen(陈立泉), Hong Li(李泓)

Chin. Phys. B . 2017, 26(7): 078201. **doi:** 10.1088/1674-1056/26/7/078201

Forming solid electrolyte interphase *in situ* in an ionic conductingLi$_{1.5}$Al$_{0.5}$Ge$_{1.5}$(PO$_4$)$_3$-polypropylene (PP) basedseparator for Li-ion batteries

Jiao-Yang Wu(吴娇杨), Shi-Gang Ling(凌仕刚), Qi Yang(杨琪), Hong Li(李泓), Xiao-Xiong Xu(许晓雄), Li-Quan Chen(陈立泉)

Chin. Phys. B . 2016, 25(7): 078204. **doi:** 10.1088/1674-1056/25/7/078204

A high-performance rechargeable Li–O_2 battery with quasi-solid-state electrolyte*

Jia-Yue Peng(彭佳悦)[1,2], Jie Huang(黄杰)[3], Wen-Jun Li(李文俊)[4], Yi Wang(王怡)[1,2], Xiqian Yu(禹习谦)[1,†], Yongsheng Hu(胡勇胜)[1], Liquan Chen(陈立泉)[1], and Hong Li(李泓)[1,2,‡]

[1] *Beijing National Laboratory for Condensed Matter Physics, Institute of Physics, Chinese Academy of Sciences, Beijing*, 100190, *China*
[2] *School of Physical Sciences, University of Chinese Academy of Sciences, Beijing* 100049, *China*
[3] *Beijing WeLion New Energy Technology Co., LTD, Beijing* 102402, *China*
[4] *Beijing Key Laboratory of Green Reaction Engineering and Technology, Department of Chemical Engineering, Tsinghua University, Beijing* 100084, *China*

(Received 1 April 2018; revised manuscript received 4 May 2018; published online 25 June 2018)

A novel transparent and soft quasi-solid-state electrolyte (QSSE) was proposed and fabricated, which consists of ionic liquid ($PYR_{14}TFSI$) and nano-fumed silica. The QSSE demonstrates high ionic conductivity of 4.6×10^{-4} S/cm at room temperature and wide electrochemical stability window of over 5 V. The Li–O_2 battery using such quasi-solid-state electrolyte exhibits a low charge-discharge overpotential at the first cycle and excellent long-term cyclability over 500 cycles.

Keywords: quasi-solid-state electrolyte, Li–O_2 battery

PACS: 82.47.Aa, 82.45.Gj, 78.55.Kz **DOI:** 10.1088/1674-1056/27/7/078201

1. Introduction

Large-scale energy storage with high energy density is of vital importance for the exploitation of renewable energy resources. Among all present electrochemical storage systems, Li–O_2 battery is a very promising candidate due to the highest theoretical energy density of 3505 Wh/kg. Li–O_2 battery utilizes the Li metal as anode and O_2 as the cathode, following the reaction route of $2Li + O_2 \rightarrow Li_2O_2$.[1,2] Up to now, mainly four types of Li–O_2 batteries have been widely investigated including aqueous, aprotic, solid-state, and mixed aqueous/aprotic based Li–O_2 batteries systems.[2] The aqueous and aprotic based Li-air battery exhibits relatively simple structure and has attracted much research attention. However, these two types of Li–O_2 batteries are still faced with many critical challenges. On Li anode side, safety concern due to Li dendrite formation and side reaction with H_2O, O_2, and CO_2 cannot be avoided. While on cathode side, electrolyte decomposition, evaporation, and reaction with O^{2-} and O_2^{2-} tend to occur.[3] Owing to the wide electrochemical window and enhanced safety property, solid-state electrolyte based Li–O_2 battery becomes a competitive candidate. Wang *et al.*[4] reported Li–O_2/air batteries using $Li_{1.3}Al_{0.3}Ti_{1.7}(PO_4)_3$ (LATP) solid electrolyte as cathode protective layer, which can prevent organic electrolyte from evaporation and decomposition. Kitaura and Zhou[5] also reported a Li–O_2 battery using $Li_{1.575}Al_{0.5}Ge_{1.5}(PO_4)_3$ (LAGP) as solid electrolyte. It can operate from room temperature to 120 °C. However, the application of all-solid-state Li-air battery is still hindered by the poor mechanical flexibility and fragile property. In addition, the large interfacial resistance between solid electrolyte and electrodes further confines the practical application.

Li–O_2 battery using quasi-solid-state electrolyte (QSSE) exhibits the combined advantages comparing to that using liquid and solid-state electrolyte, in terms of high ionic conductivity, high mechanical flexibility and superior safety characteristics. Due to its potential future development, much work has been performed to study QSSE based Li–O_2 battery in recent years. Wu *et al.*[6] reported a Li–O_2 battery using super-hydrophobic quasi-solid-state electrolyte (SHQSE) membrane, which can operate under humid atmosphere (RH = 45%) for 150 cycles. Yi *et al.*[7] proposed a Li–O_2 battery fabricated with hybrid solid electrolyte (HSE), which offered high Li^+ transfer number of 0.75 and exhibits long cyclability (> 350 cycles). Yang *et al.*[8] reported a flexible Li–O_2 battery with excellent mechanical stability and cycle performance even under various bended and twisted conditions. These pioneering works verified the advantages of QSSE based Li–O_2 battery and demonstrates its enormous potential for future applications. The key issue to realize practical QSSE based Li–O_2 battery is to fabricate QSSE with high

*Project supported by the National Key R&D Program of China (Grant Nos. 2016YFB0100300 and 2016YFB0100100), the National Basic Research Program of China (Grant No. 2014CB932300), the Beijing Municipal Science & Technology Commission, China (Grant No. D171100005517001), the Strategic Priority Research Program of the Chinese Academy of Sciences (Grant No. XDA09010000), and the National Natural Science Foundation of China (Grant No. 51502334).

†Corresponding author. E-mail: xyu@iphy.ac.cn
‡Corresponding author. E-mail: hli@iphy.ac.cn

© 2018 Chinese Physical Society and IOP Publishing Ltd

ionic conductivity and good interfacial property with cathode materials. One feasible method to fabricate QSSE is to solidify ionic liquid on nano-oxide particles by utilizing the strong confinement of ionic liquid molecules in between the oxide nanoparticles.[9] Ito *et al.*[10] prepared QSSE by compositing EMI-TFSA and nano-silica. They further fabricated a QSSE based Li–$LiCoO_2$ cell which could charge and discharge up to 10 cycles. The ionic conductivities of Li[G4]TFSI hybridized with different nano-oxide particles have been investigated by Matsuo *et al.*[11] Bipolar stacked Li–$LiFePO_4$ battery, with Li[G4]TFSI-γ-Al_2O_3 as the QSSE, demonstrates a high output potentials of 6.5 V. Unemoto *et al.*[12] further assembled a Li–S battery using IL-fumed-silica nanoparticles as the QSSE, which presents improved performance at high sulfur utilization ratios. So far, much work has been carried out on QSSE based Li–O_2 battery. However, further investigations are still needed to improve the electrochemical performances for practical applications.

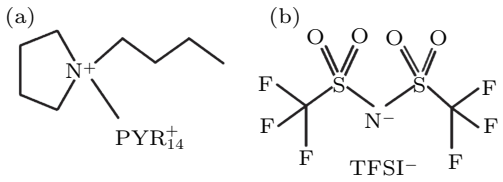


Fig. 1. The representative structure of (a) PYR_{14}^{+} and (b) $TFSI^{-}$.

In this work, we designed and prepared a novel QSSE which composite $PYR_{14}TFSI$ ionic liquid with the nano-fumed silica. The QSSE with optimal composition shows excellent ionic conductivity. A $PYR_{14}TFSI$-SiO_2-based quasi-solid-state Li–O_2 battery was assembled thereafter, which can operate at both room temperature and high temperature. With the combination of electrochemical, morphological and spectroscopic characterizations, a thorough investigation has been carried out on the $PYR_{14}TFSI$-SiO_2-based Li–O_2 batteries to understand the degradation mechanisms.

2. Experiment

2.1. Fabrication of quasi-solid electrolyte

The $LiN(SO_2CF_3)_2$ salt (LiTFSI, $>99\%$, Sigma Aldrich Co.) was heated at 120 °C in vacuum before used. The solution that contained 0.2M LiTFSI in $PYR_{14}TFSI$ was mixed with fumed silica (7 nm, Sigma Aldrich Co.) at a volume fraction 80% in methanol by stirring for 6 h. The mixed solution was then dried for 8 h at 70 °C in vacuum to get the quasi-solid electrolyte powder. Then the quasi-solid electrolyte powder was mixed with 5 wt% PTFE in an agate mortar to get the quasi-solid free-standing film. All these experiments were conducted in an-argon filled glove box at room temperature.

2.2. Preparation of the cathode electrode

The fabricated quasi-solid electrolyte powder, Ketjen Black (KB) and the PVDF binder were mixed with the weight fraction of 70:25:5 in the N-methyl-2-pyrrolidone (NMP) solvent. The slurry was pasted onto the carbon paper current collector and then dried at 120 °C under vacuum for 6 h to form the working cathode.

2.3. Li–O_2 cell assembling

The Li–O_2 battery was prepared by a Li foil with a diameter of 14 mm, the quasi-solid electrolyte film with a diameter of 16 mm and the cathode with a diameter of 14 mm. The three parts were assembled in the CR-2032 coin-type lithium-air cells in an argon-filled glove box (MBraun, H_2O and $O_2 < 0.1$ ppm). Then the cell was sealed in a glass container, which was filled with pure oxygen. Charge–discharge tests were carried out on a Land Battery Testing System. The tests were performed in the stove at 25 °C and 80 °C, respectively.

2.4. Characterization

The morphologies of the samples were characterized by field emission scanning electron microscopy (S4800, Hitachi). The XPS spectra were recorded by ESCALAB 250 Xi, Thermo Fisher with monochromatic 150 W Al Kα radiation. Before the characterization, the cathode was washed by dimethyl ether (DME) solvent for three times and dried in the vacuum for 8 h.

3. Results and discussion

The fabricated $PYR_{14}TFSI$-SiO_2 quasi-solid-state electrolyte (QSSE) film is soft and transparent as shown in inset of Fig. 2(a). The SEM image (Fig. 2(a)) indicates that the QSSE film is uniform and compact, which would be helpful for partially prohibiting the side reaction between O_2 and Li metal anode. The ionic conductivity of the QSSE was measured by conducting the Electrochemical Impedance Spectroscopy (EIS) experiment with a SS|QSSE|SS cell (SS refers to stainless steel). The conductivity has reached 4.6×10^{-4} S/cm and 6.0×10^{-4} S/cm at 25 °C and 75 °C, respectively. The QSSE with such a high ionic conductivity was suitable for the application in Li–O_2 batteries, compared to the aprotic electrolyte (2.5×10^{-4} S/cm). The Arrhenius plot of ionic conductivity of QSSE at different temperature is shown in Fig. 2(b). According to Arrhenius equation $\sigma = A/T\exp(-E_a/\kappa T)$, where σ, A, T, E_a, and κ refer to ionic conductivity, pre-exponential factor, temperature, activation energy, and Boltzmann constant, respectively, the E_a is calculated to be 0.18 eV. This value is lower than that of the traditional LAGP solid electrolyte (0.31 eV),[7] indicating a high Li^+ diffusion ability in

the QSSE. The linear sweep voltammetry (LSV) experiment was performed with a Li|QSSE|SS cell and the results are shown in Fig. 2(c). It shows that the QSSE has a wide electrochemical window (> 5.0 V), higher than the most widely-used ether-based electrolyte (usually < 4.5 V). Therefore, the as-prepared QSSE could be a suitable solid-state electrolyte for Li–O_2 batteries, which can operate in the voltage range of 2 V and 4.6 V (vs. Li/Li^+). Certainly, it can also be used for rechargeable metallic lithium batteries.

The electrochemical performances of the QSSE was evaluated in the Li–O_2 batteries. These quasi-solid-state Li–O_2 batteries can operate at both room temperature (25 °C) and high temperature (80 °C). With a current density of 100 mA/g and a lower discharge cut-off voltage of 2.2 V, the QSSE-based Li–O_2 batteries deliver a discharge capacity of 6715 mAh/g and 29942 mAh/g at 25 °C and 80 °C, respectively. The much larger discharge capacity at 80 °C is due to the higher ionic conductivity of QSSE and therefore the smaller reaction polarization in Li–O_2 battery. Figures 3(b) and 3(c) display the typical discharge-charge curve of the QSSE-based Li–O_2 batteries cycled at different current densities with a fixed capacity of 1000 mAh/g. For the electrochemical measurements at 25 °C, the Li–O_2 battery shows a smaller overpotential of 0.60 V and a higher round-trip efficiency of 80% at a lower current density of 50 mA/g, while a larger overpotential over 2.0 V and lower round-trip efficiency of at a larger current density of 500 mA/g. The rate performances are much improved at a higher temperature of 80 °C. The QSSE-based Li–O_2 batteries can work even at a current density of 2000 mAh/g, with an overpotential of only 1.5 V and round-trip efficiency of 64%. At 100 mA/g, the overvoltage between charge and discharge is only 0.45 V, and the corresponding round-trip efficiency is 85%.

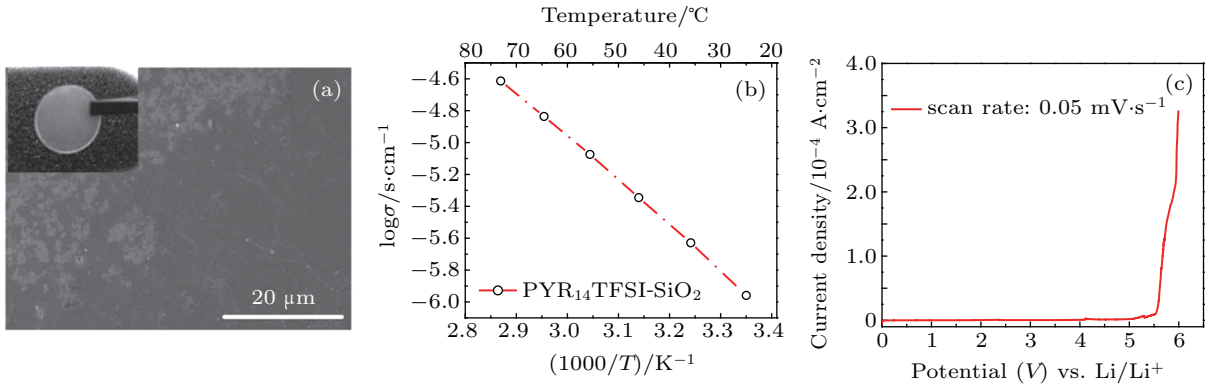


Fig. 2. (color online) Characterizations of the $PYR_{14}TFSI\text{-}SiO_2$ quasi-solid-state electrolyte (QSSE). (a) The SEM image and the optical image (inset) of the QSSE; (b) Arrhenius plots of Li ionic conductivities of the QSSE; (c) linear sweep voltammetry scan for the QSSE with a scanning rate of 0.05 mV/s.

In addition, it can be seen that the reaction polarization for the discharge process is less affected when the current density increased from 100 mA/g to 2000 mA/g, but the reaction polarization for the charge process shows the distinct increase, indicating the oxygen evolution reaction (OER) process confines the rate performance of Li–O_2 batteries. The EIS spectra of the QSSE-based Li–O_2 batteries operated at 80 °C (Fig. 3(d)) shows a large increase in impedance after the first discharge and significant decrease after the first charge process. The increase of the impedance can be ascribed to the accumulation of discharge product of Li_2O_2, which is an electronic insulator. After the first recharge process, the majority of the discharged products decompose and the resistance of the cell significantly decreases (20 ohm but still larger than that of the original cell), indicating a good reversibility of the QSSE-based Li–O_2 with controlled discharged capacity. The cycle performances were also evaluated by charging and discharging the cells with a fixed capacity of 1000 mAh/g. The cells can charge and discharge for 100 and 500 cycles at a current density of 100 mA/g and 1000 mA/g at 25 °C and 80 °C, respectively (Figs. 3(e) and 3(f)). The terminal voltage, reflecting the reaction polarization, gradually increases upon prolonged cycling. This is likely due to the accumulation of discharge products and inactive products from side reactions.

In order to investigate the morphology changes of the electrode after the charge-discharge process, SEM measurements were performed. A relatively smooth surface can be observed for the pristine electrode as shown in Figs. 4(a) and 4(d). After the first discharge process, a large cluster of toroid-shaped particles can be observed on the surface of cathode electrode (Figs. 4(b) and 4(e)), implying the high utilization of void volume in the cathode electrode. The formation of large toroid-like particles, consisting of small plates, is started at the active sites of KB[13,14] and then grows layer-by-layer through a solution-mediated electrochemical process[15] driven by the partial solubility of discharge intermediate LiO_2 in $PYR_{14}TFSI$. Figures 4(c) and 4(f) show that after the first recharge process, large toroid-shaped clusters disappear, but numerous small flake-shaped particles still exist on the surface of cathode, indicating that the discharge products can only be partially decomposed.

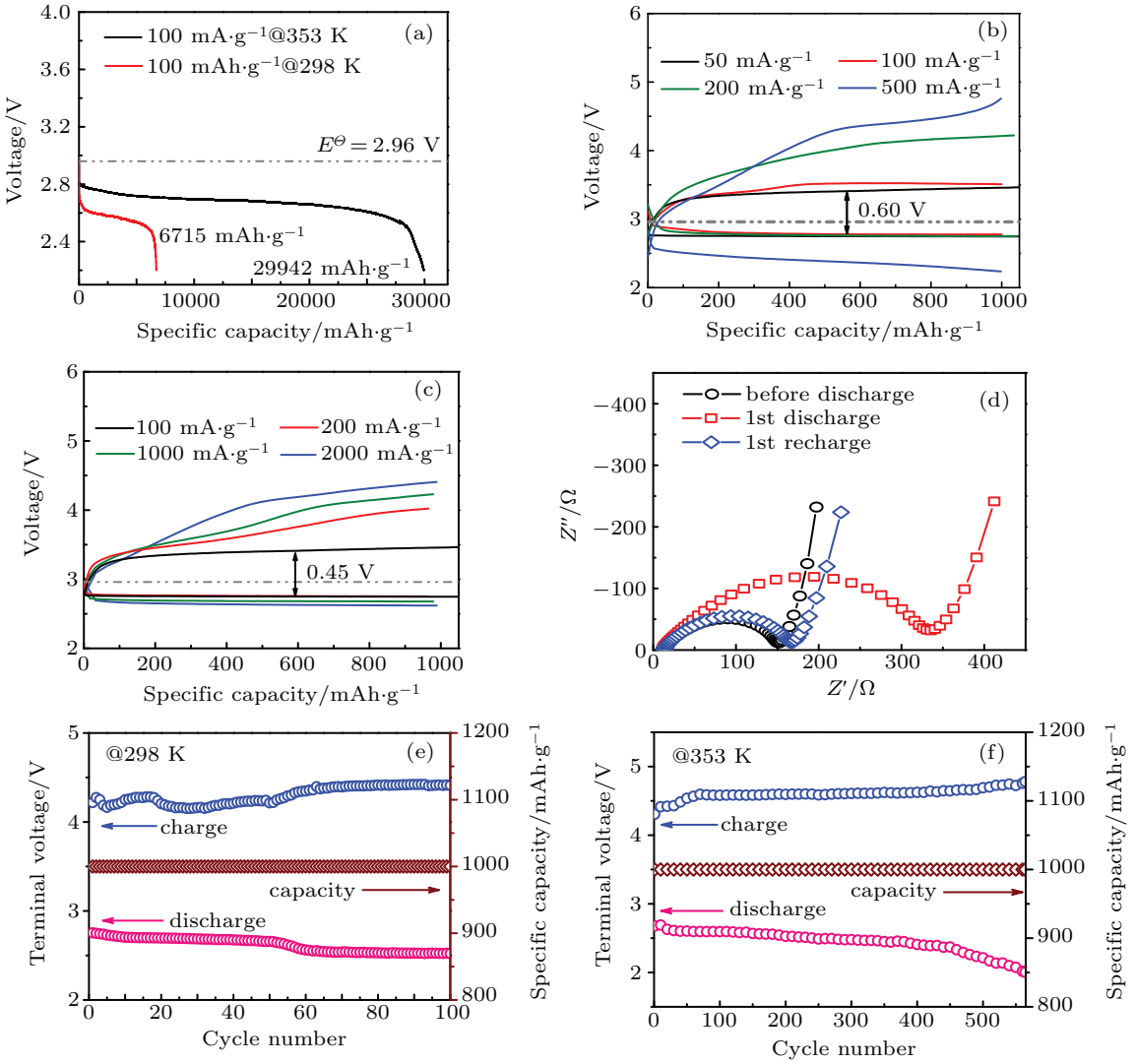


Fig. 3. (color online) Electrochemical performances of the QSSE-based Li–O_2 battery. (a) Charge-discharge curves measured at a current density of 100 mA/g with discharge cut-off voltage of 2.2 V at 25 °C and 80 °C; (d) EIS spectra of the QSSE-based Li–O_2 battery measured before and after the first discharge and charge process. A current density of 100 mA/g with a fixed capacity of 1000 mAh/g was used for Li–O_2 cell cycled at 80 °C; typical discharge-charge profiles of Li–O_2 cells cycled with a fixed capacity of 1000 mAh/g at (b) 25 °C and (c) 80 °C, respectively; the terminal voltage recorded with Li–O_2 cells cycled at (e) 25 °C and (f) 80 °C, respectively.

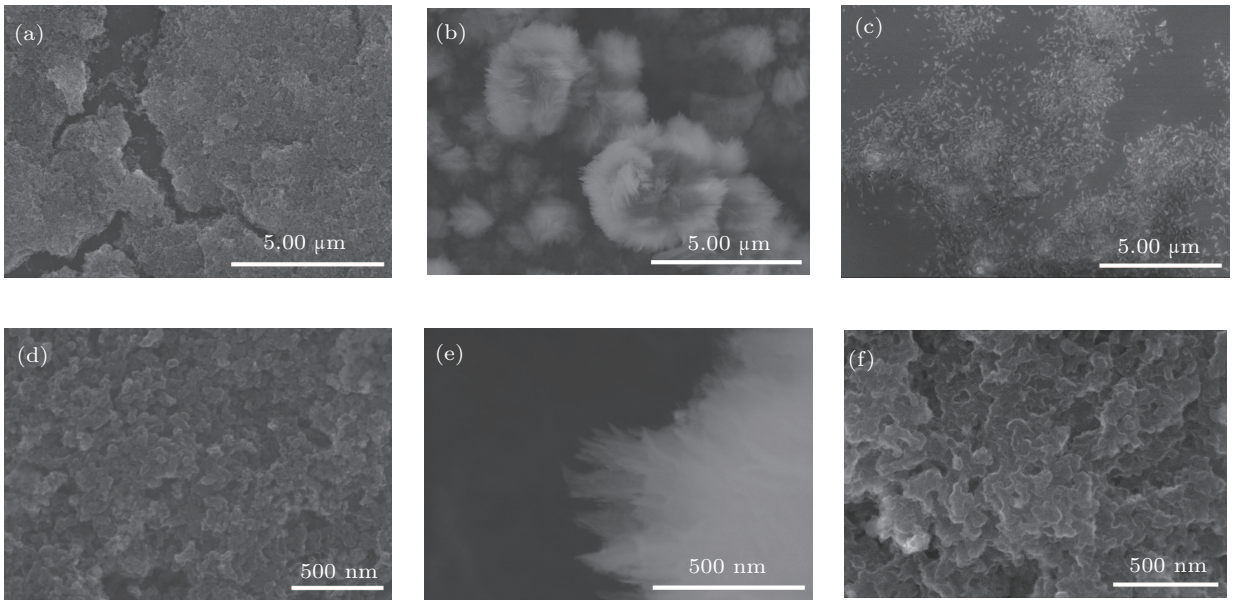


Fig. 4. The SEM images of the cathode electrode at ((a), (d)) pristine, ((b), (e)) first discharge, and ((c), (f)) first charge states. The Li–O_2 battery was tested at a current density of 100 mA/g with a fixed capacity of 1000 mAh/g at 80 °C.

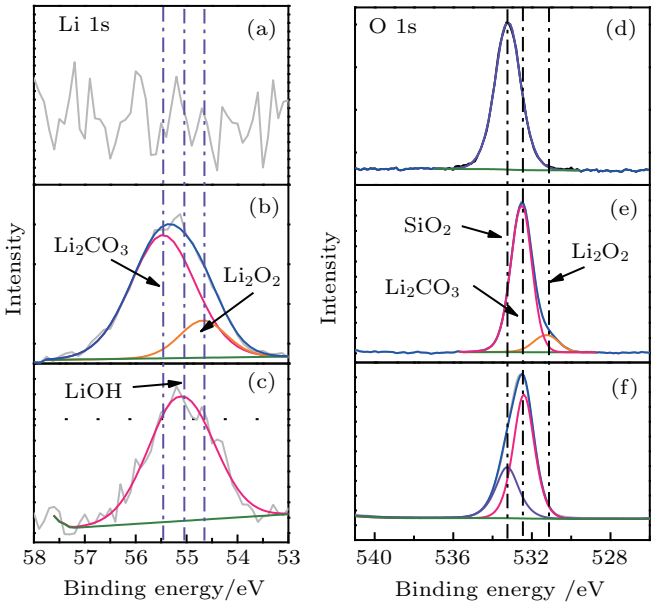


Fig. 5. (color online) The (a, b, c) Li 1s and (d, e, f) O 1s XPS spectra collected on cathode electrodes at pristine, first discharge and first charge states, respectively. The Li–O_2 battery was tested at a current density of 100 mA/g with a fixed capacity of 1000 mAh/g at 80 °C.

Figure 5 shows the Li 1s and O 1s XPS spectra measured on the cathode electrode before and after charge and discharge processes. The peak located at ∼ 533.2 eV on O 1s XPS spectrum of pristine electrode can be assigned to SiO_2. After the first discharge process, SiO_2 signal disappears, while two new peaks appear. These two new peaks, located at ∼ 531.0 eV and ∼ 532.5 eV, can be assigned to Li_2O_2 and Li_2CO_3,[16] respectively. This indicates that the formation of a thick layer of discharge products on the cathode electrode. The formation of Li_2O_2 and Li_2CO_3 can be further confirmed by Li 1s spectrum, where the two peaks at ∼ 54.6 eV and ∼ 55.5 eV can be ascribed to Li_2O_2 and Li_2CO_3,[16] respectively. Therefore, the discharge process can be summarized to follow the reaction of $2Li + O_2 \rightarrow Li_2O_2$, while the formation of Li_2CO_3 is due to the side reaction: $2Li_2O_2 + 2C + O_2 \rightarrow 2Li_2CO_3$.[17] After the first recharge process, the peaks of Li_2O_2 on the O 1s and Li 1s spectra disappear, indicating the decomposition of Li_2O_2 during the charging process. However, the peak assigned to Li_2CO_3 can still be observed, indicating that the Li_2CO_3 is only partially decomposed. A new peak, located at ∼ 55.0 eV, can be identified and assigned to LiOH. The appearance of LiOH indicates another route of side reaction: $2Li_2O_2 + 2H_2O \rightarrow 4LiOH + O_2$, where H_2O might come from O_2 gas. The accumulation of side reaction products leads to the increase in charge–discharge overpotential, which is the main reason for performance degradation of Li–O_2 batteries.

4. Conclusion

In summary, a quasi-solid-state electrolyte (QSSE), made by mixing ionic liquid with nano-fumed SiO_2 particles (80:20 v/v), was successfully fabricated. This electrolyte shows a wide electrochemical window up to 5.5 V. The ionic conductivity of the QSSE is 4.6×10^{-4} S/cm and 6.0×10^{-4} S/cm at 25 °C and 75 °C, respectively. The superior ionic conducting properties guarantee the electrochemical performances of the Li–O_2 battery. The overpotential for the first cycle was only 0.6 V and 0.45 V, and the round-trip efficiency was 80% and 85.8%, for Li–O_2 batteries tested at 25 °C and 80 °C, respectively. Although the reaction kinetics and reversibility have been greatly improved, the capacity degradation cannot be avoided owing to the insufficient decomposition of discharge products and side reactions. Therefore, substantial efforts are still needed for further improving the cycle performance of Li–O_2 batteries.

References

[1] Bruce P G, Freunberger S A, Hardwick L J and Tarascon J M 2012 *Nat. Mater.* **11** 19
[2] Girishkumar G, Mccloskey B, Luntz A C, Swanson S and Wilcke W 2010 *J. Phys. Chem. Lett.* **1** 2193
[3] Li F, Kitaura H and Zhou H 2013 *Energy Environ. Sci.* **6** 2302
[4] Wang X, Zhu D, Song M, Cai S, Zhang L and Chen Y 2014 *ACS Appl. Mater. Interfaces* **6** 11204
[5] Kitaura H and Zhou H 2015 *Sci. Rep.* **5** 13271
[6] Wu S, Yi J, Zhu K, Bai S, Liu Y, Qiao Y, *et al.* 2017 *Adv. Energy Mater.* **7** 1601759
[7] Yi J, Liu Y, Qiao Y, He P and Zhou H 2017 *ACS Energy Lett.* **2** 1378
[8] Yang X Y, Xu J J, Chang Z W, *et al.* 2018 *Adv. Energy Mater.* 1702242
[9] Shimano S, Haoshen Zhou A and Honma I 2007 *Chem. Mater.* **19** 5216
[10] Ito S, Unemoto A, Ogawa H, Tomai T and Honma I 2012 *J. Power Sources* **208** 271
[11] Matsuo T, Gambe Y, Sun Y and Honma I 2015 *Sci. Rep.* **4** 6084
[12] Unemoto A, Ogawa H, Gambe Y and Honma I 2014 *Electrochim. Acta* **125** 386
[13] Mitchell R R, Gallant B M, Yang S H and Thompson C V 2013 *J. Phys. Chem. Lett.* **4** 1060
[14] Griffith L D, Sleightholme A E S, Mansfield J F, Siegel D J and Monroe C W 2015 *ACS Appl. Mater. Interfaces* **7** 7670
[15] Aetukuri N B, McCloskey B D, García J M, Krupp L E, Viswanathan V and Luntz A C 2015 *Nat. Chem.* **7** 50
[16] Guéguen A, Novák P and Berg J 2016 *J. Electrochem. Soc.* **163** A2545
[17] Mccloskey B D, Speidel A, Scheffler R, Miller D C, Viswanathan V, Hummelshøj J S, *et al.* 2012 *J. Phys. Chem. Lett.* **3** 997